A MULTISCALE MODEL FOR MODAL ANALYSIS OF COMPOSITE STRUCTURES WITH BOLTED JOINTS

Z. Zhang[1], Y. Xiao*[2], Y. Z. Shen[3] and Z.Q. Su[4]

[1, 2,3] School of Aerospace Engineering and Applied Mechanics, Tongji University, 1239 Siping Road, Shanghai, P.R. China
[1, 4] Department of Mechanical Engineering, The Hong Kong Polytechnic University, Hong Kong, P.R. China
[1]Email: 2013_tjzhangzhen@tongji.edu.cn
[2*]Email: y_xiao@tongji.edu.cn
[3]Email: shenyuanzhen11@163.com
[4]Email: zhongqing.su@polyu.edu.hk

Keywords: Bolted composite joint, Residual torque, Resonant frequency, Damping ratio, Fractal contact theory, Complex eigenvalue method

ABSTRACT

A new finite element(FE) model considering surface roughness of contact interfaces in a bolted composite joint, consist of laminated composite beams and fasteners (i.e., bolt, nut and gasket) along with thin-layer interfaces, was developed to model the dynamic response of the bolted joint. The macro-properties of the thin-layer interfaces were derived through micro-analysis on the single-asperity contact in conjunction with fractal contact theory. Firstly, normal (i.e., storage normal modulus) and tangential contact stiffness (including both storage and loss tangential modulus) of a single-asperity contact was expressed with external loads and surface properties of the contact interface, according to Hertzian contact theory and Mindlin micro-slip model, respectively. Subsequently, the contact stiffness of the interfaces which feature a multi-asperity contact in the micro perspective, subject to different pressure, was derived by integrating the contact stiffness of single asperity in the contact region. The damping and the stiffness of the composite structures with bolted joints were modelled using frequency-dependent modulus using complex eigenvalue method that were implemented in ABAQUS FE code. Predicted damping ratio and resonant frequency of the bolted composite joint under different residual torques were examined by comparing with the experimental investigation. Results from theoretical prediction and experiment are in good consistency, which shows resonant frequency for a bolted joint decreases whereas damping ratio increases with a reduce in the residual torque applied on the bolt.

1 INTRODUCTION

To meet the requirement of structural integrity and sustainability, a large variety of composite and metallic structural members are assembled in terms of bolted joints. For instance, approximately three million fasteners are used to assemble more than 130,000 parts in a Boeing 777 airplane [1]. However, the friction at the bolted interfaces, viscoelasticity and ageing of joining materials, adverse working conditions, can initiate the preload relaxation of a bolt and subsequently accelerate the bolt loosening [2]. Therefore, it is of highly importance to develop reliable techniques capable of identifying the occurrence and degree of bolt loosening in a bolted composite joint at an early stage.

The present study proposed a multiscale FE model to model the dynamics of the joint under different residual torques involving in roughness of the contact surfaces by using complex eigenvalue method [3]. Firstly, the applied torque of the joint was theoretically correlated with contact stiffness of the interface according to fractal contact theory [4]. Based on the developed interfacial contact model in terms of pressure-dependent stiffness, the FE model of the joint was built and utilized to calculate dynamic responses of the joint. The numerically predicted relation between the residual torque and modal parameters of the joint was further validated by experimental investigation.

2 FRACTAL CONTACT MODEL

Surfaces of solid are uneven in the micro perspective with randomly distributed asperities, as shown in Figure 1. Fractal geometry method can be used to characterize rough surface without independence on the resolution and sampling length of measuring instrument.

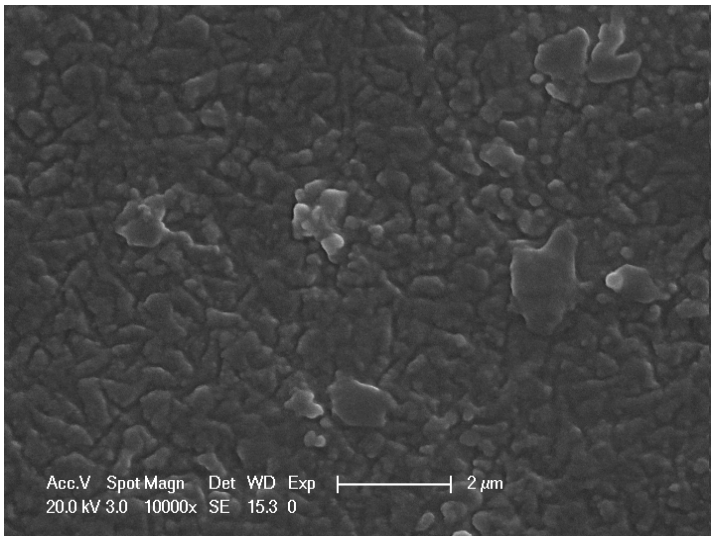

Figure 1: Asperities on the surface of a composite beam.

In the fractal contact model, asperity contacts with different sizes undergo deformation of different degree and feature distinct contact areas. Large asperities in contact form contact areas exceeding the critical area (a_c), which distinguishes elastic and plastic deformation, therefore undergo an elastic deformation. While asperity contacts with small sizes are in a plastic deformation. For asperities undergo the elastic deformation, the reliance of contact load (p_e) and contact stiffness (normal stiffness k_n^e and tangential stiffness k_t^e) on the contact area (a') can be expressed as

$$p_e = \frac{4}{3(2\pi)^{0.5}} E' G^{D-1} a'^{(3-D)/2} \tag{1}$$

$$k_n^e = 2E' (\frac{a'}{2\pi})^{0.5} \tag{2}$$

$$k_t^e = \frac{8G' a'^{0.5}}{(2\pi)^{0.5}} (1 - \frac{T}{\mu P})^{1/3} \tag{3}$$

where D and G denote fractal dimension and roughness, respectively. E' and G' are the equivalent Young's and shear modulus of two rough surfaces in contact, respectively. T represents tangential load and P normal force applied on the contact asperities. μ signifies the friction factor.

While for asperities in the plastic deformation, contact load (p_p) and contact stiffness (normal stiffness k_n^p and tangential stiffness k_t^p) can be expressed as

$$p_p = \frac{1}{2} H a' \tag{4}$$

$$k_n^p = k_t^p = 0 \tag{5}$$

The size (i.e., contact area) distribution of contact spots is written as

$$n(a') = \frac{D}{2}\psi^{(2-\mathrm{D})/2} a_l'^{\mathrm{D}/2} a'^{-(\mathrm{D}+2)/2} \tag{6}$$

where ψ is the domain extension factor and a_l' the largest truncated area of contact asperities.
The total normal load (P) applied on the surface can subsequently be obtained by using the size distribution, as

$$\begin{aligned} P &= \int_{a_c'}^{a_l'} p_e n(a')\,\mathrm{d}a' + \int_{a_s'}^{a_c'} p_p n(a')\,\mathrm{d}a' \\ &= \begin{cases} \dfrac{2^{0.25}}{\sqrt{\pi}} E G^{0.5} \psi^{0.25} a_l^{0.75} \ln \dfrac{a_l}{a_c} + 6H\psi^{0.25} a_l^{0.75} a_c^{0.25} & (\mathrm{D}=1.5) \\ \psi^{1-0.5D}\left[\dfrac{2^{3-0.5D} E D G^{(\mathrm{D}-1)}}{3(3-2D)\sqrt{\pi}} a_l^{0.5D}(a_l^{1.5-D} - a_c^{1.5-D}) + \dfrac{2DH}{2-D} a_l^{0.5D} a_c^{1-0.5D}\right] & (\mathrm{D}\neq 1.5) \end{cases} \end{aligned} \tag{7}$$

The normal and tangential contact stiffnesses are evaluated as

$$K_n = \int_{a_c'}^{a_l'} k_n n(a')\,\mathrm{d}a' = \frac{2E'D}{\sqrt{\pi}(1-\mathrm{D})}\psi^{1-0.5D} a_l^{0.5D}(a_l^{0.5-0.5D} - a_c^{0.5-0.5D}) \tag{8}$$

$$K_t = \int_{a_c'}^{a_l'} k_t n(a')\,\mathrm{d}a' = \frac{8G'\psi^{1-0.5D} D a_l^{0.5D}(a_l^{0.5-0.5D} - a_c^{0.5-0.5D})}{\pi^{0.5}(1-D)}\left(1-\frac{T}{\mu P}\right)^{1/3} \tag{9}$$

When tangential slip occurs between contact asperities, tangential damping ratio can be obtained as

$$\eta = \frac{12\left\{1-\left(1-\frac{T}{\mu P}\right)^{\frac{5}{3}} - \frac{5T}{6\mu P}\left[1+\left(1-\frac{T}{\mu P}\right)^{\frac{2}{3}}\right]\right\}}{\pi\left\{3+2\left(1-\frac{T}{\mu P}\right)^{\frac{5}{3}} - 5\left(1-\frac{T}{\mu P}\right)^{\frac{2}{3}}\right\}} \tag{10}$$

Therefore, the complex contact modulus in the normal and tangential direction can be written as follows:

$$K_n^* = K_n \tag{11}$$

$$K_t^* = K_t + i\eta K_t \tag{12}$$

3 NUMERICAL ANALYSIS

Based on the fractal model of interfacial contact stiffness, finite element analysis using thin-layer elements, as depicted in Figure 2, is introduced in this section. The orthotropic stiffness matrix for the thin-layer elements has the following form:

$$[K] = \begin{bmatrix} 0 & 0 & 0 & 0 & 0 & 0 \\ 0 & 0 & 0 & 0 & 0 & 0 \\ 0 & 0 & K_n^* & 0 & 0 & 0 \\ 0 & 0 & 0 & 0 & 0 & 0 \\ 0 & 0 & 0 & 0 & K_t^* & 0 \\ 0 & 0 & 0 & 0 & 0 & K_t^* \end{bmatrix} \tag{13}$$

The complex modulus method is also used to describe the properties of composite material. The frequency-dependent damping ratio of composite material is ascertained through impact tests on three

types of unidirectional (namely 0, 45, 90 degree) composites with different lengths. The dependence of material damping ratio on the frequency can be expressed as

$$\eta_0 = 4.6249 \cdot 10^{-4} + 1.5593 \cdot 10^{-6} \cdot f \tag{14}$$

$$\eta_{45} = 1.3798 \cdot 10^{-3} + 4.62379 \cdot 10^{-4} \cdot f \tag{15}$$

$$\eta_{90} = 1.038 \cdot 10^{-3} + 4.6961 \cdot 10^{-4} \cdot f \tag{16}$$

When modelling a bolted composite joint with different torques remained on the bolt, the contact stiffness matrix defined in Equation (13) is adjusted according to Equations (8) and (9). C3D8 elements and tie contact are used in the ABAQUS model. Complex frequency method is adopted to calculate the resonant frequency and damping ratio of the bolted composite joint under different applied torques.

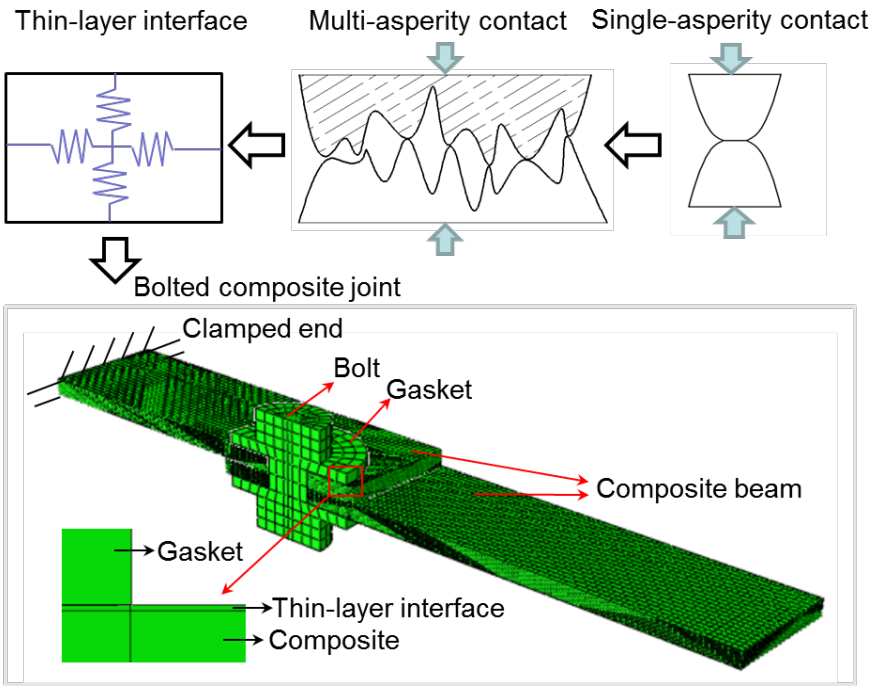

Figure 2: FE model of a bolted composite joint with thin-layer interfaces.

4 EXPERIMENTAL VALIDATION

To validate the numerical analysis regarding dynamic responses of the bolted composite joint with distinct leftover torques, vibration modal parameters, including both resonant frequency and damping ratio are comparatively obtained from impact tests on the joint. The beam specimens were cut from sheets of laminated T700/7901 carbon-fiber-reinforced epoxy, obtained using hot pressing with a stacking sequence $[90, 0]_{4s}$. Specimens were 2 mm thick and 30 mm wide. A composite beam with a length of 50 mm was assembled with another beam with a length of 70 mm. The setup for the modal test is shown in Figure 3, which is consist of test specimens, fixtures, a displacement sensor (Donghua 5E106) and a dynamic strain indicator (Donghua 5923N). The joint was clamped vertically with one end fixed (i.e., the beam with a length of 50 mm) by the fixtures. During the test, impact forces were applied at different points of the specimen and the displacement meter was used to measure the displacement response of the joint at a sampling frequency of 10 kHz.

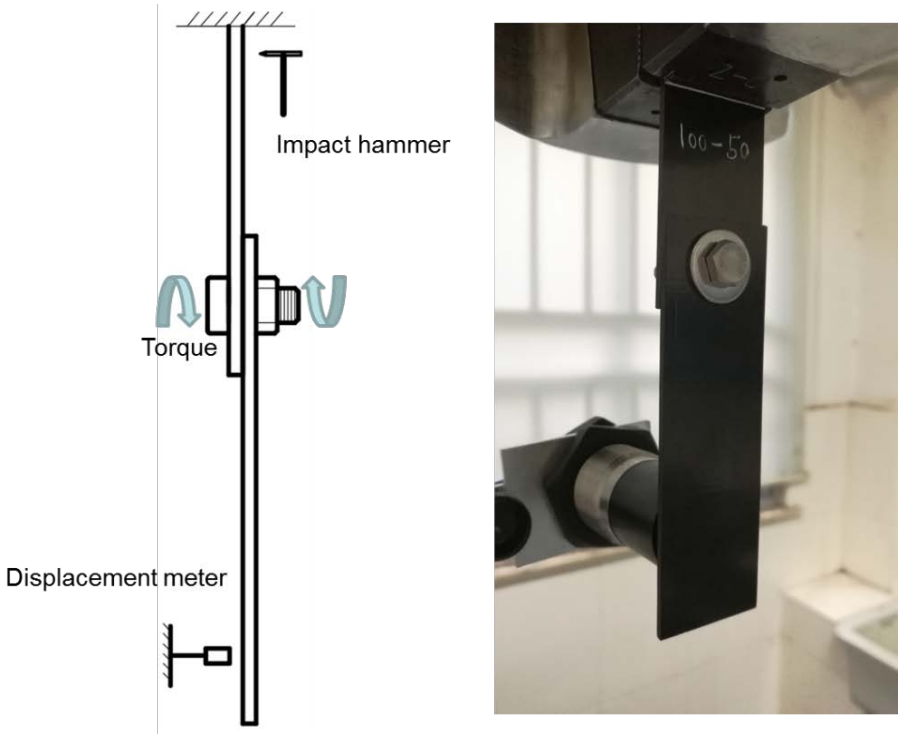

Figure 3: Schematic illustration of impact test of a bolted composite joint

The representative free decay curve of the joint upon subject to an impact force is shown in Figure 4. The damping ratio of the joint is ascertained by fitting the envelope of the free decay curve and the resonant frequency is obtained by processing Fast-Fourier-Transform on the curve. For the sake of avoiding involvement of air damping, which is linearly dependent on the excitation magnitude, damping ratios of the joint subject to varied excitation intensity are obtained. Subsequently, the intercept of the curve, which represents damping ratio of the joint measured from a "zero" excitation magnitude, is taken as damping ratio of the joint in this study.

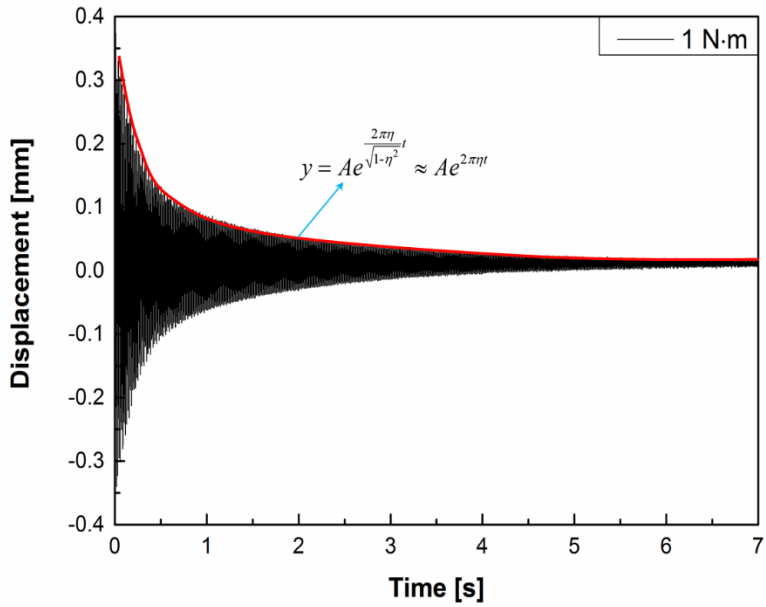

Figure 4: Free decay curve regarding response displacement of a joint subject to an impact force

5 RESULTS AND CONCLUSONS

Observations on the experimental results of the bolted composite joint under varied torques measured from impact tests (see Figure 5) indicate that resonant frequency of the bolted composite joint decreases whereas damping ratio increases with a reduce in the leftover torque applied on the bolt. Damping ratio decreases starting at 1 N·m until the applied torque reaches 11 N·m, after which it presents an increasing trend. Whereas, resonant frequency increases starting from 1 N·m until a preload of 9 N·m is reached, after which it stabilizes with increase in preload. This implies that pressure applied on the joining material induced by a torque of 9 N·m is close to or exceeds the compressive yield strength of connecting material in the thickness direction. Comparison between numerical analysis and experimental investigation reveals that the proposed multiscale model accurately predicts the modal parameters of bolted joints under different residual torque. The reduce in resonant frequency of a bolted composite joint upon the occurrence of bolt loosening can be attributed to the decrease of the normal and tangential contact stiffness at the contact interface and the augment in damping ratio is caused by the increase of the tangential energy dissipation between the contact surfaces.

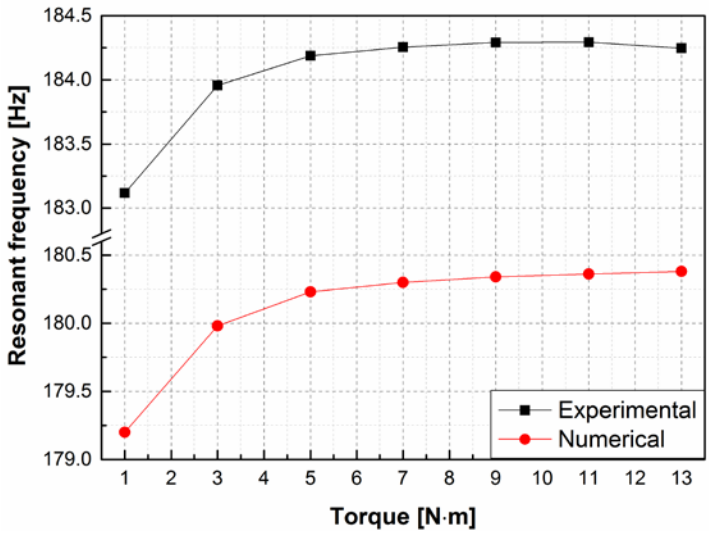

(a)

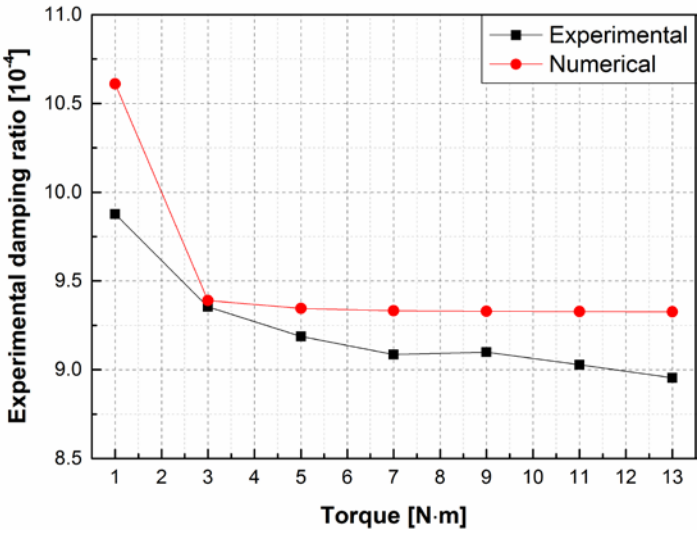

(b)

Figure 5: (a) Resonant frequency and (b) damping ratio *vs.* residual torque of a bolted composite joint.

REFERENCES

[1] Z. Zhang, M. L. Liu, Z. Q. Su and Y. XIAO. Quantitative evaluation of residual torque of a loose bolt based on wave energy dissipation and vibro-acoustic modulation: A comparative study. *Journal of Sound and Vibration*, **383**,2016, pp.156-170 (doi: 10.1016/j.jsv.2016.07.001).

[2] Z. Zhang, Y. Xiao, Y. Q. Liu and Z. Q. SU. A quantitative investigation on vibration durability of viscoelastic relaxation in bolted composite joints. *Journal of Composite Materials*, **50**(29), 2016, pp.4041-4056(doi: 10.1177/0021998316631810).

[3] R. M. Crane and J. W. Gillespie. Characterization of the vibration damping loss factor of glass and graphite fiber composites. *composites science and technology*, **40**(4), 1991, pp.355-375. (doi: 10.1016/0266-3538(91)90030-S).

[4] S. Wang and K. Komvopoulos. A fractal theory of the interfacial temperature distribution in the slow sliding regime: Part I—elastic contact and heat transfer analysis. *Journal of Tribology*, **116**(4), 1994, pp.812-822 (doi: 10.1115/1.2927338).